

Fachhochschule Dortmund

Institut für die Digitalisierung von Arbeits- und Lebenswelten (IDiAL)

# Developing a Rover-Following Application for APPSTACLE

RESEARCH PROJECT

*Author*

Daniel Paredes

*Supervisor*

Robert Höttger

December 22, 2018

# Contents

<b>Abstract</b>	<b>2</b>
<b>1 Introduction</b>	<b>3</b>
1.1 APPSTACLE . . . . .	3
1.2 Eclipse Kuksa . . . . .	3
1.3 In-vehicle Platform (Rover) . . . . .	5
1.4 Rover Services . . . . .	5
1.5 Rover Application . . . . .	6
<b>2 Design and Implementation</b>	<b>7</b>
2.1 Use case description . . . . .	7
2.2 Requirements . . . . .	7
2.3 Camera calibration and the pinhole model . . . . .	8
2.4 Extrinsic Parameters . . . . .	11
2.5 Rotation matrix to Euler angles . . . . .	11
2.6 Use case implementation details . . . . .	12
<b>3 Experimental Results</b>	<b>20</b>
3.1 Known distance and angle . . . . .	20
3.2 Difference between ultrasonic sensor and camera . . . . .	21
<b>4 Challenges and issues</b>	<b>22</b>
4.1 Estimation of extrinsic parameters . . . . .	22
4.2 Camera vision field . . . . .	22
4.3 Maximum detectable rotations . . . . .	22
4.4 Problems measuring distance traveled . . . . .	24
4.5 Switching to Raspbian to AGL . . . . .	24
<b>Conclusions</b>	<b>26</b>
<b>A Appendix</b>	<b>31</b>
A.1 Calibration of the picam in raspbian . . . . .	31
A.2 Answer to the “Life, the Universe, and All” questions . . . . .	31

# Abstract

The purpose of this research project is to develop an application for Rover in-vehicle platform in the context of APPSTACLE project and Eclipse Kuksa ecosystem. The application allows a Rover to follow without human intervention a visual marker on another Rover. `OpenCV` libraries and Eclipse Kuksa services are the main building blocks of the application.

Our experimental results show the accuracy of the application to estimate and reach the target position. Moreover, we described challenges and issues related to our application and how to address them.

# Chapter 1

## Introduction

Today automotive software-intensive systems are developed in silos by each car manufacturer or original equipment manufacturer (OEM) in-house [13] and this approach is not suitable for long-term challenges in the industry. For example, big data simulations and virtual modeling can lower development costs and speed up time to market, embedded data sensors should enable more precise monitoring of the performance of vehicles and components [10], and the car should be connected not only to monitor working parts and safety conditions around it, but also to communicate with other vehicles and with an increasingly intelligent roadway infrastructure [11].

### 1.1 APPSTACLE

APPSTACLE or *open standard APplication Platform for carS and TrAnsportation vehiCLES* is an international ITEA research project that aims at providing standardize platform for car-to-cloud connectivity, external cloud or in-vehicle applications and the use of open source software without compromising safety and security [13]. This document describes an in-vehicle application based on the open source software developed throughout the project.

### 1.2 Eclipse Kuksa

The result of APPSTACLE project is *Eclipse Kuksa* and it provides an example tooling stack for the connected vehicle domain [12]. The Eclipse Kuksa ecosystem consists of an in-vehicle platform, a cloud platform, and an app development IDE as shown in figure 1.1.

It is possible to collect, store and analyze data through the different Kuksa layers of the in-vehicle platform. These layers are: *meta-kuksa* adds the kuksa in-vehicle applications into the AGL image, *meta-kuksa-dev* contains all extra packages that are useful for the development process but aren't required in the production Image, and *meta-rover* holds all the needed packages to enable the development for the Rover [12]. The in-vehicle platform runs on top of *Automotive Grade Linux* or AGL which is an open-source project from The Linux Foundation. The goal of AGL is to develop a GNU/Linux based operating system and a framework for automotive applications [6].

The development of Eclipse Kuksa plug-ins or applications can be done using the web-

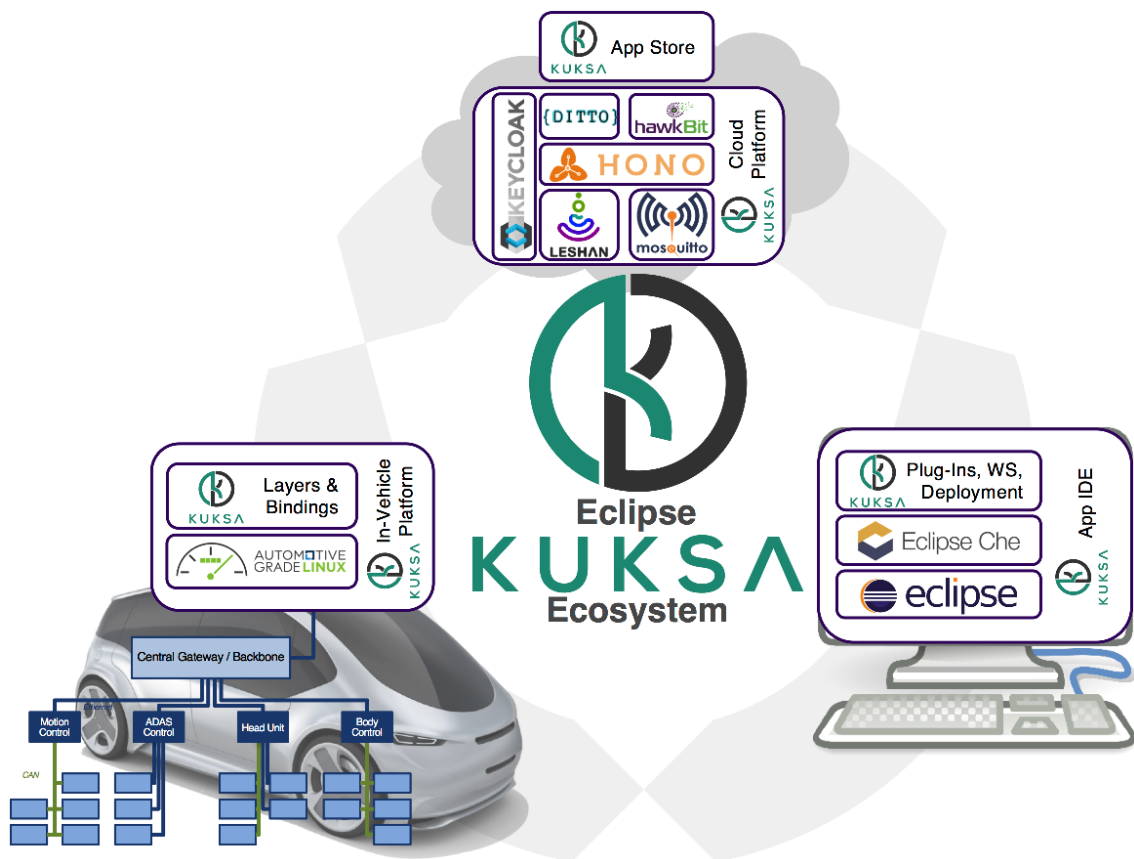


Figure 1.1: Eclipse Kuka Ecosystem [12]

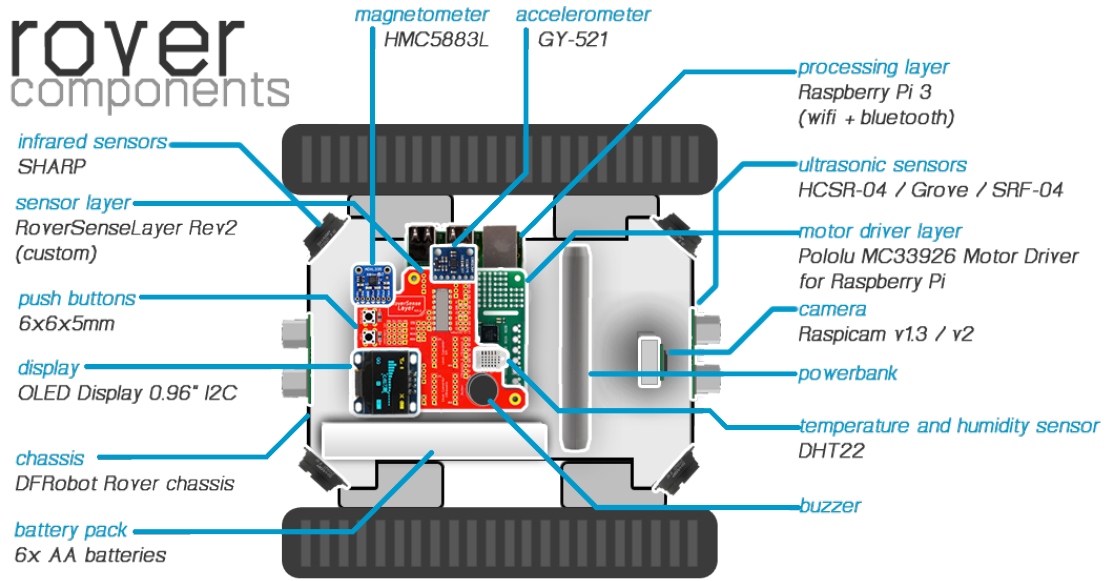


Figure 1.2: Rover Components [1]

browsed based IDE known as *Eclipse Che*. In order words, a complete toolchain is available as extensions to *Eclipse Che* which allows not only a fast, but also and independent platform development.

In addition, the cloud platform is built on top of other Eclipse frameworks such as Eclipse Hono used in telemetry applications and Eclipse Ditto used to create a digital rover twin; and also provides the Kuksa app-store, so users could download an app and deploy it directly in their rovers.

### 1.3 In-vehicle Platform (Rover)

The in-vehicle platform or Rover is based on a raspberry pi 3 that can run *Raspbian Jessie* or *AGL* as Operating system. The available hardware is shown in figure 1.2. There are two layers besides the raspberry pi. The *Motor driver* layer based on a MC33926 Motor Driver, and the *Sense* layer, a custom made circuit board that is designed as a shield on top of MC33926 [1]. The Sense layer provides interfaces for sensors (accelerometers, magnetometer, infrared, ultrasonic, humidity and temperature), buttons, buzzer and OLED display.

### 1.4 Rover Services

Rover Services are modules that runs on Linux-based embedded single board computers. These services provide interfaces to interact with the in-vehicle hardware (sensors, camera, motors, buttons, buzzer) and cloud communication. One can think of services as libraries of an operation system which can be used for software development.

In the context of Eclipse Kuksa, new services can be added using a model-based approach using raml files containing information about hardware to be used and interfaces with its

inputs and outputs. The `Raml2ag1` tool [4] will generate the basic structure of required C++ files. Once the services is complete, it's compiled and added to the operating system libraries.

An example RAML file is shown below:

```
title: Rover Hello World
mediaType: application/json
version: v1
types:
  rover_sensor_id:
    enum:
      - front
      - rear
  rover_demo_id:
    enum:
      - driving
      - infrared
/print_hello_world:
  description: "Service test"
```

## 1.5 Rover Application

It is possible to develop applications in Eclipse Kuksa based on rover services, these applications are called rover-apps. The development of rover-apps can be done locally on the user's laptop or desktop or on *Eclipse Che*. In this research project, we developed a rover-app for following without human intervention a visual marker on another Rover. Our application is based on `OpenCV` libraries, and camera, driving and sensor services. In addition, the development of our application was done locally because `OpenCV` is not integrated on the AGL software development kit embedded in Eclipse Che toolchain.

Finally, let us explain the organization of this research project. In chapter 2 we present design and implementation of our rover-app with some theoretical background. In chapter 3 experimental results are given. In chapter 4 we describe challenges and issues that should be addressed in further versions. At the of the document we summarize the conclusions.

## Chapter 2

# Design and Implementation

### 2.1 Use case description

In this research project we develop a use case for rover-apps. For the use case we are using two *Rovers*, a **Rover Leader** and a **Rover Follower**. Hereinafter, we will only use **Leader** or **Follower** to refer to them. The leader has a visual marker, the follower should detect it, estimate the angle  $\beta$  and distance  $d$  with respect to the leader as is shown in figure 2.1, and follow the leader.

This chapter will be focused on the development of the behavior of the follower because is the only rover that must be completely autonomous. The following sections will describe requirements, main hardware parts involved and software tools required to implement follower's behavior, camera calibration and pose estimation theory, and software implementation details.

### 2.2 Requirements

The main requirements for the rover follower are listed in table 2.1.

Table 2.1: Most importante requirements

Requirement	Description
Detect visual marker	The follower should detect an Aruco Marker using the PiCamera mounted on it. The camera field of vision should contain the marker, and this one should be within 100cm of radius.
Estimation angle and distance	The follower should estimate the angle and distance to the marker every time the leader moves to another position.
Follower driving	The follower should steer based on the estimated values. It should first rotate based on the estimated angle, and then drive forward based on the estimated distance, but it should stop when is within 5cm of radius from the leader.



Requirement	Description
Leader movement	The leader should only move to a new position when the follower reaches it.
Autonomous driving	The follower should be completely autonomous. Detection of the marker and driving should be done with no human intervention other than turning on the rover and initial positioning.
Operating system	The follower should run Raspbian Jessie as operation system.
OpenCV library	The follower should use OpenCV 3.4.1 [3] for the video processing including reading video frames, marker detection, and estimation of the angle and distance to the marker.
Rover-App library	The follower code should be based on the services such as sensor reading and driving provided by the rover-app library.
Maintainability	The follower code should be maintainable following principles of modularity and encapsulation, and avoiding code duplication code.
Reusable	The follower code should be reusable. Subroutines or functions should be well defined, and it's design should take into account orthogonality and extensibility.
Understandability	The follower code should be understandable. Comments should be relevant, variable and function names should be self explanatory, the code sections should be well defined (includes, global/static/volatile variables declarations, function definitions, main function).

### 2.3 Camera calibration and the pinhole model

Camera calibration is a necessary step in 3D computer vision in order to extract metric information from 2D images [15]. If you hold that box in front of you in a dimly lit room, with the pinhole facing some light source you see an inverted image appearing on the translucent plat [5]. In figure 2.2, a 3D object (pyramid) is projected first on a scene plane, and then on the image plane. Each point in the scene plane or *world frame* will have it's correspondence in the image plane or *camera frame*. The distance from the pinhole to the image plane is called focal length.

The mathematical model of a pinhole camera can be derived using linear algebra and the visual representation shown in figure 2.2.

Let's denote a 2D point  $\hat{\mathbf{m}} = [x, y, 1]^T$ , a 3D point  $\hat{\mathbf{M}} = [X, Y, Z, 1]^T$ , there exists a camera projection matrix  $\mathbf{P}$  such that  $\hat{\mathbf{m}} = \mathbf{P}\hat{\mathbf{M}}$ .

$$\hat{\mathbf{m}} = \mathbf{P}\hat{\mathbf{M}} = \mathbf{A}[\mathbf{R} \quad \mathbf{t}]\hat{\mathbf{M}} \quad (2.1)$$

The camera intrinsic matrix  $\mathbf{A}$  contains information about the internal parameters of

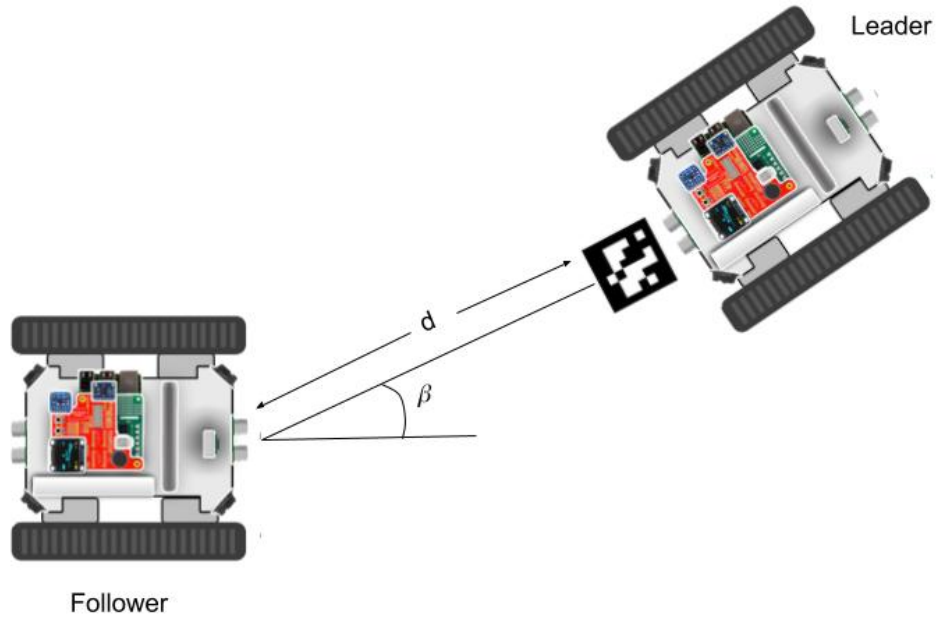


Figure 2.1: Rover Use Case

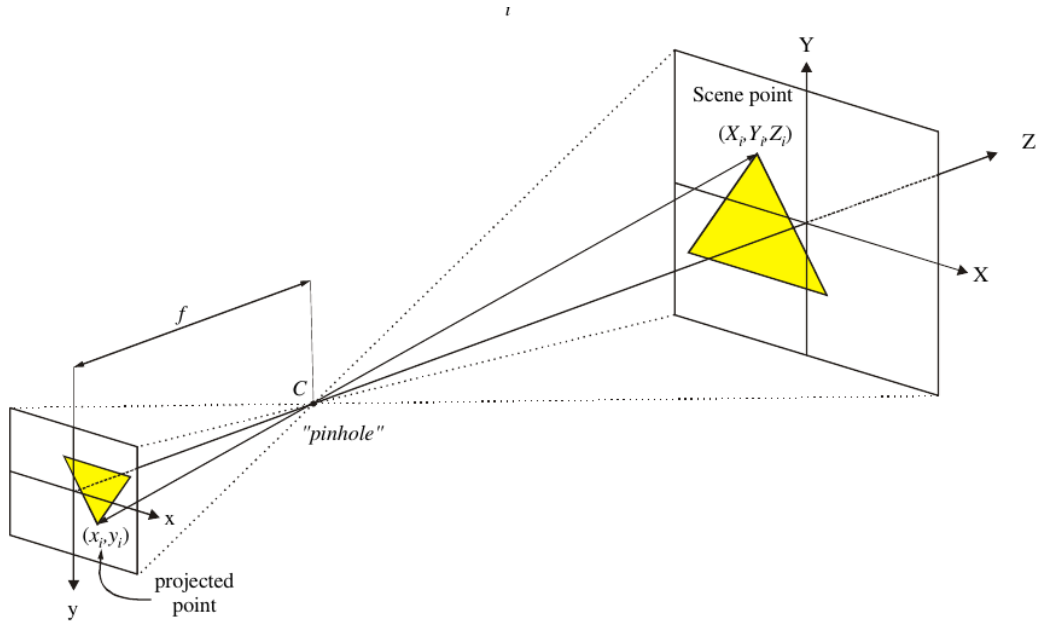


Figure 2.2: The pinhole imaging model [8].

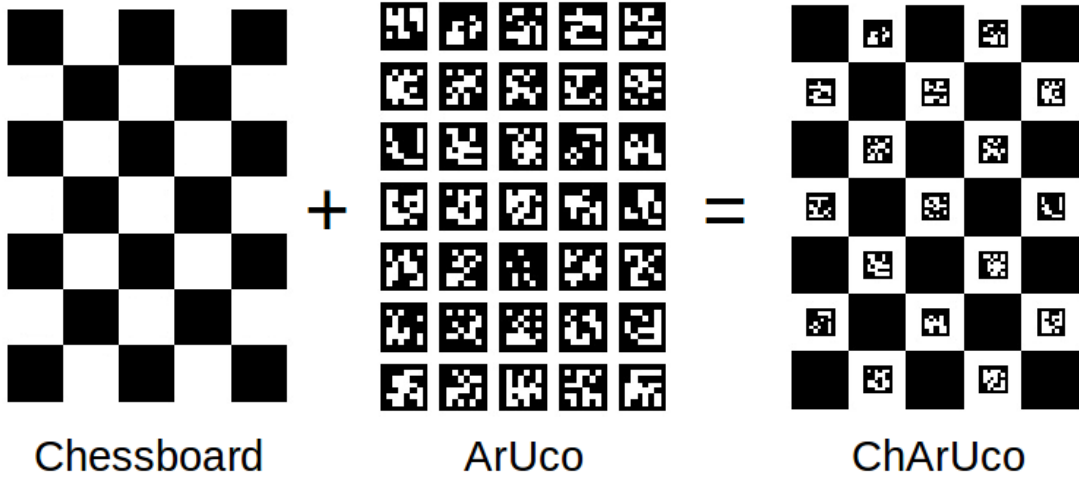


Figure 2.3: Planar Patterns [3]

the camera: focal length, image sensor format and principal point or image center. The coordinates of the principal point is described by  $(x_0, y_0)$ ,  $\alpha_x$  and  $\alpha_y$  represent the focal length in terms of pixels on the axis  $x$  and  $y$ , and  $\gamma$  is the skew of image.

$$\mathbf{A} = \begin{bmatrix} \alpha_x & \gamma & x_0 \\ 0 & \alpha_y & y_0 \\ 0 & 0 & 1 \end{bmatrix} \quad (2.2)$$

The camera extrinsic parameters are given by the rotation matrix  $\mathbf{R}$  and translation vector  $\mathbf{t}$ , which are used to project an image on the world frame to camera frame. There is also a scale transformation, but it's already given by  $\alpha_x$  and  $\alpha_y$ .

Current cameras are equipped with lenses that produce some distortions on the images, however, the pinhole model is still a good approximation for our case since we are using a **PiCamera** which has minimal distortions.

The camera calibration has been done with using **OpenCV**. This library implementation is based on the technique described by [16] and the matlab implementation done by [9]. The calibration technique in [16] requires the camera to observed a planar pattern, usually a chessboard pattern, at different orientations, the more the better the estimation of the intrinsic parameters. The calibration algorithm minimize the reprojection error which is the distance between observed feature points on the planer pattern and the projected using the estimates parameters.

For calibration we used a *ChArUco* board instead of the classical chessboard because it generates a better estimation of the parameters [3].

The procedure to calibrate the PiCamera is straightforward with **OpenCV** and the sample codes found under `opencv_contrib-3.4.1/modules/aruco/samples`. **A detailed explanation can be found in the Appendix (not sure but is a remainder).**

1. Create a charuco board, print it and paste it on a solid and planar surface.

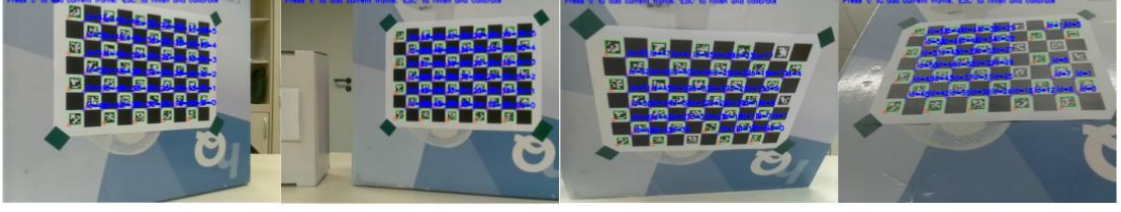


Figure 2.4: Some camera views used for calibration

2. Compile the example code `calibrate_camera_charuco.cpp` and run it
3. Place your pattern in different orientations and take pictures
4. When you are done, just close the program

In our case, the camera intrinsic matrix  $\mathbf{A}$  is as following:

$$\mathbf{A} = \begin{bmatrix} \alpha_x & \gamma & x_0 \\ 0 & \alpha_y & y_0 \\ 0 & 0 & 1 \end{bmatrix} = \begin{bmatrix} 6.125e+02 & 0. & 3.216e+02 \\ 0 & 6.122e+02 & 2.365e+02 \\ 0 & 0 & 1 \end{bmatrix} \quad (2.3)$$

## 2.4 Extrinsic Parameters

As it was mention before, the camera extrinsic parameters are given by the rotation matrix  $\mathbf{R}$  and translation vector  $\mathbf{t}$ . A rotation matrix can be formed as the product of three rotations around three cardinal axes, e.g.,  $x$ ,  $y$ , and  $z$ , or  $x$ ,  $y$ , and  $x$ . This is generally a bad idea, as the result depends on the order in which the transforms applies [14].

However, a rotation can be also represented by a rotation axis  $\mathbf{k} = [k_x, k_y, k_z]^T$  and an angle  $\theta$ , or equivalently by a vector  $\omega = \theta\mathbf{k}$ . In order to do the transformation from axis-angle representation to rotation matrix, the cross-product matrix  $\mathbf{K}$  and Rodrigues' rotation formula can be used.

$$\mathbf{K} = \begin{bmatrix} 0 & -k_z & k_y \\ k_z & 0 & -k_x \\ -k_y & k_x & 0 \end{bmatrix} \quad (2.4)$$

$$\mathbf{R} = \mathbf{I} + (\sin \theta)\mathbf{K} + (1 - \cos \theta)\mathbf{K}^2 \quad (2.5)$$

## 2.5 Rotation matrix to Euler angles

In order to get the angles related a rotation whose yaw, pitch and roll angles are  $\phi$ ,  $\rho$  and  $\psi$ . These angles are rotations in  $z$ ,  $y$  and  $x$  axis respectively. We will rotate first about the  $x$ -axis, then the  $y$ -axis, and finally the  $z$ -axis. Such a sequence of rotations can be represented as the matrix product

$$\mathbf{R} = R_z(\phi) R_y(\rho) R_x(\psi) \quad (2.6)$$

$$R_x(\psi) = \begin{bmatrix} 1 & 0 & 0 \\ 0 & \cos \psi & -\sin \psi \\ 0 & \sin \psi & \cos \psi \end{bmatrix} \quad (2.7)$$

$$R_y(\rho) = \begin{bmatrix} \cos \rho & 0 & \sin \rho \\ 0 & 1 & 0 \\ -\sin \rho & 0 & \cos \rho \end{bmatrix} \quad (2.8)$$

$$R_z(\phi) = \begin{bmatrix} \cos \phi & -\sin \phi & 0 \\ \sin \phi & \cos \phi & 0 \\ 0 & 0 & 1 \end{bmatrix} \quad (2.9)$$

Given the given sequence of rotations and the algorithm described by [7], the angles can be found using algorithm 1.

```

if  $R_{31} \neq \pm 1$  then
  |  $\phi = \arctan 2(R_{21}, R_{11})$ 
  |  $\rho = -\arcsin(R_{31})$ 
  |  $\psi = \arctan 2(R_{32}, R_{33})$ 
else
  |  $\phi = 0$ 
  |  $\rho = -R_{31}\pi/2$ 
  |  $\psi = \arctan 2(-R_{23}, R_{22})$ 
end
Algorithm 1: Slabaugh's algo-
rithm

```

## 2.6 Use case implementation details

As it was mentioned before, the follower should be completely autonomous. In order to do so, the follower will need to read data from sensors, process that data and generate movement based on the processed data.

In figure 2.1 is shown a diagram of our use case. The main sensor is a PiCamera, the processing part performs the marker detection on the captured frames and the calculation of the Euler angles and distance based on the equations described in the last section, and finally the movement is generated using the driving rover services.

### Video Processing with OpenCV

Just like in the case of camera calibration, we use **OpenCV** and the submodule **aruco** to capture video and process the frames in order to extract information from the visual markers. To estimate and detect the marker at the beginning we should load the camera intrinsic parameters, saved in a YAML file, and the Aruco dictionary, composed by 250 markers and a marker size of 6x6 bits [3], to memory.

```

// cameraMatrix: camera intrinsic parameters
// dictionary: aruco dictionary
cv::FileStorage fs("calibration.yml", cv::FileStorage::READ);
fs["camera_matrix"] >> cameraMatrix;
cv::Ptr<cv::aruco::Dictionary> dictionary =
    cv::aruco::getPredefinedDictionary(cv::aruco::DICT_6X6_250);

```

Given a video frame, it is possible to detect Aruco markers if they are visible. When the marker is detected, we extract the four corners of the marker using `cv::aruco::detectMarkers` function. The first corner is the top left corner, followed by the top right, bottom right and bottom left. The next step is to estimate the extrinsic camera parameters, which means the rotation vector  $\omega$  and the translation vector  $\mathbf{t}$ . The size of the marker is an input parameter of the `OpenCV` function `cv::aruco::estimatePoseSingleMarkers`. In our case the marker size is 7cm.

```

// image: input frame
// corners: detected corners
// rvec: rotation vector
// tvec: translation vector
cv::aruco::detectMarkers(image, dictionary, corners, ids);
cv::aruco::estimatePoseSingleMarkers( corners, 0.07,
                                     cameraMatrix, 0, rvec, tvec);

```

The next step is calculating the Euler angles by using function `cv::Rodrigues` and Slabaugh's algorithm. The `cv::Rodrigues` function is a direct implementation of equations ?? and ??.

```

// rmat: rotation matrix
// angle: Euler angles
cv::Rodrigues(rvec.row, rmat);
rotationMatrixToEulerAngles(rmat, angle)

```

An example is shown in figure 2.5, the Euler angles are  $\psi = 165$ ,  $\rho = 25$  and  $\phi = 0$ . The green, red and blue axes correspond to the X-axis, Y-axis and Z-axis respectively. As expected from the pin hole model,  $\psi$  is near 180 because the image is facing the camera as result the blue axis points towards the camera.

A basic code for video processing the marker is as follows:

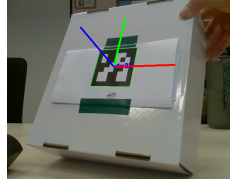


Figure 2.5: Camera axis

```
// Initialization
cv::VideoCapture inputVideo(0);
cv::FileStorage fs("calibration.yml", cv::FileStorage::READ);
fs["camera_matrix"] >> cameraMatrix;
fs["distortion_coefficients"] >> distCoeffs;

inputVideo.open(0);
cv::Ptr<cv::aruco::Dictionary> dictionary =
    cv::aruco::getPredefinedDictionary(cv::aruco::DICT_6X6_250);
...

// Video processing
inputVideo.read(image);
cv::aruco::detectMarkers(
    image, dictionary, corners, ids);
cv::aruco::estimatePoseSingleMarkers(
    corners, 0.07, cameraMatrix,
    distCoeffs, rvec, tvec);
cv::Rodrigues(rvec, rmat);
rotationMatrixToEulerAngles(rmat, angles);
```

However, the estimated angles can not be used directly because estimations have small errors. In figure 2.6 can be observed the values of the rotation angles in a span of 1000 samples and in table 2.1 the statistics of those samples. The ground truth values for Euler angles were  $[0, 0, 0]$ , and for distance were 47.5 and 16 centimeters respectively.

Table 2.2: Statistics of estimated Euler angles and distance to visual marker

Data	Mean	$\sigma$	Median
$\psi$ deg	0.719853	0.162262	0.723000
$\rho$ deg	0.584508	0.165382	0.507618
$\phi$ deg	1.155499	0.046940	1.157000
$d$ cm	45.51706	0.033564	45.50772
$d$ cm	15.65339	0.007401	15.65401

The results of standard deviation  $\sigma$  from table 2.2 suggest the estimated values can be stable ( $\sigma < 0.16$  deg) overall, particularly in the case of distance to the marker ( $\sigma < 0.04$  cm). However, figure 2.6 suggests the existence of spike values, thus we must filter the samples in order to minimize the effect of those outliers. A median filter is highly effective removing

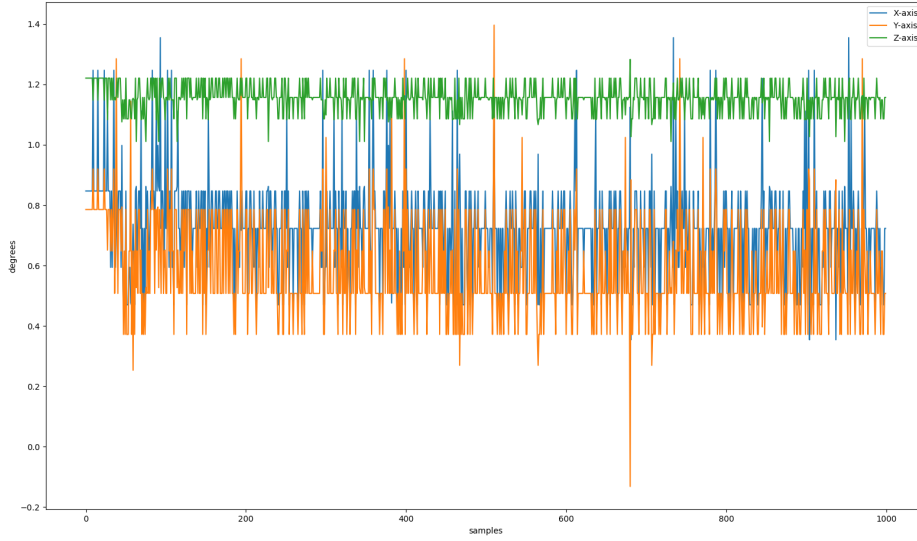


Figure 2.6: Angles in X-axis  $\psi$ , Y-axis  $\rho$  and Z-axis  $\phi$

showed that the mean and the median of Euler angles are similar, thus it is reasonable to think that outliers has small influence on the data. In other words, the mean filter is a simple and effective option against outliers problem. Its implementation is straightforward and requires no memory to save previous values. A pseudocode is as follows:

```
estAngle = 0;
for( i=0; i<samples; i++)
    estAngle += new_value;
estAngle /= samples;
```

### Rover rotations

Rover is a ground vehicle which means that only steer in one axis. Thus, only rotations in Y-Axis are possible. As shown in figure 2.7 rotations in X-axis are not possible since the rover can not fly or go underground. The same applies to rotations in Z-axis. In other words, the only relevant information from the estimated Euler angles is  $\rho$ , or the angle related the Y-axis.

### Measuring angular displacement

In order to move the follower to a defined angular position, the CY-521 board is used. The CY-521 has an accelerometer and a gyroscope. The accelerometer works by measuring the components of gravity in the different axis, taking the “earth” or gravity acceleration as reference. On the other hand, the gyroscope measures angular speed relative to itself or own rotation, using the inertial force called the Coriolis effect.



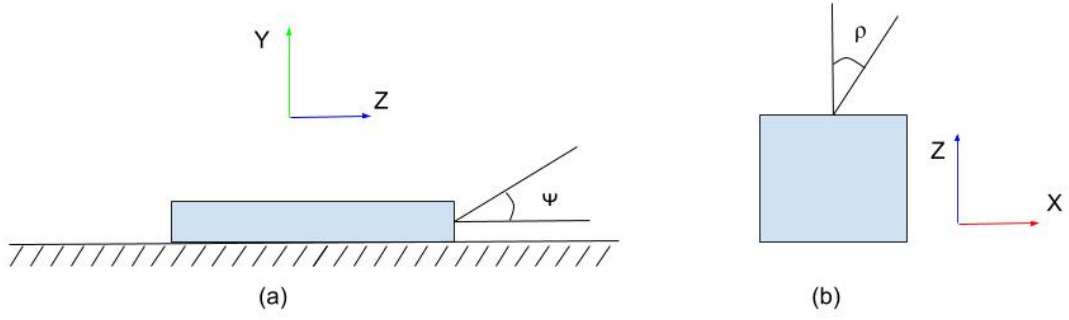


Figure 2.7: Rotation rotations (a) Rotation in X-axis (b) Rotation in Y-axis

With that information we could estimate the angular position of follower. However, the values from the accelerometer are not taking into account because the gravity vector is parallel to the Y-axis. It is important to note that we want to measure relative rotations, thus in the initial position the angle will always be 0.

The gyroscope measures angular speed in all axis, in particular the angular speed in Y-axis or  $\omega_y$ . The angular displacement  $\rho$  is just the integral of  $\omega_y$ .

$$\rho = \int \omega_y(t) dt \quad (2.10)$$

$$\omega_y = \frac{\delta \rho}{\delta t} \quad (2.11)$$

Nonetheless, the calculation is done in a computer, thus we use the *Forward Euler Method* to solve the integral.

$$\rho[n+1] = \rho[n] + \Delta t \omega_y[n] \quad (2.12)$$

where  $\Delta t$  is the sampling period between sensor readings and  $\rho[0] = 0$ . A pseudocode of the rotation routine is as follows:

```
current_angle = 0;

// clockwise rotation
if( desired_angle <= 0 ) turnRight();
// counterclockwise rotation
else turnLeft();

while( abs(current_angle - desired_angle) > 0)
    wait(sampling_period);
    current_angle += getAngle()*sampling_period;

stop();
```

### Camera Projection and rover driving

As mentioned at the beginning of this chapter, in the pin hole camera model the 2D point  $\hat{\mathbf{m}}$  and the 3D  $\hat{\mathbf{M}}$  are related through a projection matrix  $\mathbf{P}$ , and the camera projection matrix  $\mathbf{P}$  is formed by the combination of extrinsic and intrinsic camera parameters. In order to move the follower to the leader position, we must find  $\hat{\mathbf{M}}$  given  $\hat{\mathbf{m}}$ .

$$\hat{\mathbf{m}} = \mathbf{P}\hat{\mathbf{M}} = \mathbf{A}[\mathbf{R} \ \mathbf{t}]\hat{\mathbf{M}} \quad (2.13)$$

$$\mathbf{P} = \overbrace{\mathbf{A}}^{\text{Intrinsic Matrix}} \times \overbrace{[\mathbf{R} \ \mathbf{t}]}^{\text{Extrinsic Matrix}} \quad (2.14)$$

$$m_{2D} = \mathbf{A}^{-1}\hat{\mathbf{m}} = \mathbf{R}\hat{\mathbf{M}} + \mathbf{t} \quad (2.15)$$

The  $m_{2D}$  is used by `OpenCV` to estimated rotation and translation vectors. In addition,  $[\mathbf{R} \ \mathbf{t}]\hat{\mathbf{M}}$  becomes  $\mathbf{R}\hat{\mathbf{M}} + \mathbf{t}$  because the last element of  $\hat{\mathbf{M}}$  is 1. Si

$$\mathbf{R}^{-1}(m_{2D} - \mathbf{t}) = \hat{\mathbf{M}} \quad (2.16)$$

Since rotation matrix is orthogonal:

$$\mathbf{R}^T(m_{2D} - \mathbf{t}) = \hat{\mathbf{M}} \quad (2.17)$$

Thus, the rover follower first should drive forward and then rotate in order to reach to leader position. On the other hand, since the follower only rotates in Y-axis we only need to change the direction of the rotation and translation.

$$R_y(\rho) = \begin{bmatrix} \cos \rho & 0 & \sin \rho \\ 0 & 1 & 0 \\ -\sin \rho & 0 & \cos \rho \end{bmatrix} \quad (2.18)$$

$$R_y(\rho)^T = R_y(-\rho) \quad (2.19)$$

### Implementation

The activity diagram of use case is shown in figure 2.8. First, the rover API is initialized, it also includes the motor and sensors, and the camera intrinsic parameters are load into memory as described before.

```
RoverBase r_base; /* Rover API */
RoverDriving r_driving; /* Rover driving service */
RoverGY521 r_accel; /* gyro and accelerometer */
/* Ultrasonic sensors */
```

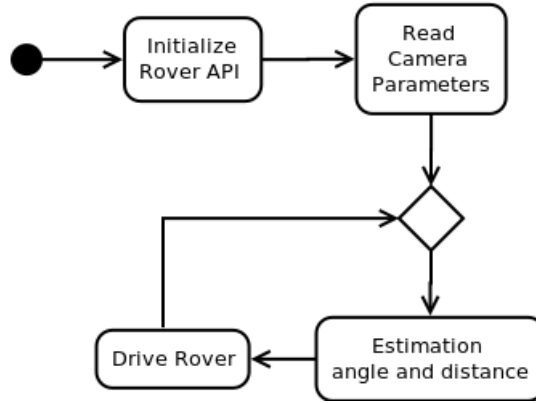


Figure 2.8: Activity diagram

```

RoverHCSR04 r_front = RoverHCSR04(ROVER_FRONT);
RoverHCSR04 r_rear  = RoverHCSR04(ROVER_REAR);

```

After the initial set up, a infinity loop starts. During the loop we estimate the angle  $\rho$  and distance  $d$ , the later is the norm of the translation vector  $d = \|\mathbf{t}\|_2$ . The motion is done in two steps: rotation and translation. The follower goes forward  $d$  centimeters, and when it is done, it rotates  $\rho$  degrees. The current distance is measured using the front ultrasonic ranging module HC-SC04. The rover-API can only give accurate information for distances lower than 40 cm [2], for distances greater than 40cm the API returns always 40cm. However, when the follower approaches the leader eventually will be in the measurable range.

Once the follower reaches the leader, it stops and wait until the leader moves again. A pseudocode of the loop is as follows:

```

while(1){
    // Initialization of the current values
    estimated_angle = 0;
    estimated_distance = 0;

    // Mean filter
    for(i=0; i<nSamples; i++){
        readFrame();
        [rvec, tvec] = getExtrinsicParameters();
        estimated_angle += getYrotation(rvec);
    }
    estimated_angle /= nSamples;
    estimated_distance = norm(tvec);

    // Driving routines

```

```
    moveForwoard(estimated_distance);  
    rotateNdegrees(estimated_angle);  
}
```

## Chapter 3

# Experimental Results

In this chapter, we evaluate the behavior of the follower in an controlled environment. We present the results of three test cases: known distance and angle and difference between ultrasonic sensor and camera. Our experiments consisted in three steps: set a known initial and final position, turn on the follower rover, measure the deviation from expected final position We measured the deviation using the front ultrasonic sensor, the PiCamera and a ruler with smallest division of the scale of 1 mm, or estimated uncertainty of 0.5 mm.

### 3.1 Known distance and angle

In this test case we evaluated followers accuracy to reach the desired position and orientation. The different setting and initial camera estimations are presented on table 3.1. Distance values are in centimeters (cm) and angle values are in degrees. For the initial position, the results show that absolute error for both distance and angle are less than 4cm and  $3^\circ$  respectively, and that relative error are less than 5% for distance and less than 9% for angle if we ignore the relative error for  $0^\circ$ .

Table 3.1: Initial settings and estimations

	1	2	3	4	5
Distance	70	70	70	70	100
Est. Distance	73.48	71.64	73.42	71.70	103.37
Absolute Error	3.48	1.64	3.42	1.70	3.37
Relative Error	4.97%	2.34%	4.89%	2.43%	3.37%
Angle $\rho$	$30^\circ$	$-30^\circ$	$16^\circ$	$-16^\circ$	$0^\circ$
Est. Angle $\rho$	$32.43^\circ$	$-27.47^\circ$	$15.78^\circ$	$-15.73^\circ$	$-2.84^\circ$
Absolute Error	$2.43^\circ$	$2.53^\circ$	$0.22^\circ$	$0.27^\circ$	$2.84^\circ$
Relative Error	8.1%	8.43%	1.38%	1.69%	$\infty$

In table 3.2 are presented the results for the final position. The absolute error for distance is less than 0.7cm, and less than  $2.75^\circ$  for angle. On the other hand, the relative error for distance and angle is, in the worst case, 14.17% and 257.89% respectively.

Table 3.2: Measurements and final estimations

	1	2	3	4	5
Distance	4.8	4.2	8.8	5.2	5.90
Est. Distance	5.48	4.64	9.50	5.72	6.44
Absolute Error	0.68	0.44	0.70	0.52	0.54
Relative Error	14.17%	10.48%	7.95%	10.00%	9.15%
Aprox. Angle $\rho$	1.54°	2.75°	1.71°	0.95°	2.10°
Est. Angle $\rho$	3.58°	5.50°	2.62°	3.40°	2.25°
Absolute Error	2.04°	2.75°	0.91°	2.45°	0.15°
Relative Error	132.47%	100%	53.22%	257.89%	7.14%

Relative error values in the final position are bigger than in the initial position because the values of distance and angle are lower. However, absolute error values have improved in the case of distance, reducing from 3.48cm to 0.7cm, and have kept stable in the case of angle.

### 3.2 Difference between ultrasonic sensor and camera

Ultrasonic sensor are commonly used to measure the distance to an object. We wanted to compare the accuracy of the ultrasonic ranging module HC-SC04 with PiCamera. In table 3.3 are presented the results of our experiments. The results show the chosen ultrasonic sensor is useless for distances larger than 40cm, while camera estimations have absolute errors lower than 1.52 cm. In [2] is mentioned that for distances greater than 40cm the sensor readings are not reliable. On the other hand, for distances smaller than 40cm both, ultrasonic readings and camera estimations, presented absolute errors lower than 0.72cm and 1cm respectively.

Table 3.3: Accuracy comparison between ultrasonic ranging module HC-SC04 readings and PiCamera estimations.

	1	2	3	4	5	6
Distance	70	50	20	15	13	4.8
PiCamera	71.52	51.24	20.32	15.41	13.72	5.48
Absolute Error	1.52	1.24	0.32	0.41	0.72	0.68
Relative Error	2.17%	2.48%	1.60%	2.73%	5.54%	14.17%
Ultrasonic	40.00	40.00	20.00	14.00	13.00	5.00
Absolute Error	30	10	0	1	0	0.2
Relative Error	42.86%	20.00%	0%	6.67%	0%	4.17%

## Chapter 4

# Challenges and issues

In this chapter we will describe open challenges and unresolved issues that should be addressed or taken into account in further versions of the described rover-app. We describe the following issues and challenges: extrinsic parameters estimation, limited camera vision field, marker maximum detectable rotation, error measurements in the current distance sensing system, and migration from Raspbian to AGL.

### 4.1 Estimation of extrinsic parameters

We should always remember that pinhole model. The *world frame* or plane is projected onto the *image frame* or plane. In figure 4.1 is presented a marker in three different positions. Rotation and translation vectors are the same for each position, because from the perspective of the camera they belong to the same world plane, thus rotation and translation vectors in all the cases are the same.

### 4.2 Camera vision field

The PiCamera mounted on the Rover has a limited vision field. As observed in figure 4.2, the PiCamera can only sense from  $-33$  degrees up to  $28$  degrees for a radius of  $50\text{cm}$ , in other words the vision field has  $-33$  degree limit on the left side and  $28$  degree limit on the right side. We could consider the vision field as a trapezoid as in figure 4.1.

Thus, the closer the marker to the camera the less vision field due to pinhole model and image projections. In addition, The limits are not the same because the PiCamera is not perfectly aligned with Rover axis.

### 4.3 Maximum detectable rotations

There is a maximum  $\rho$  angle in clockwise and counterclockwise directions that can be detected. In figure 4.3 is shown the position and angle in which the marker can still be detectable. For counterclockwise rotations the maximum  $\rho$  angle is  $-77$  degrees and for clockwise rotations is  $72$  degrees.

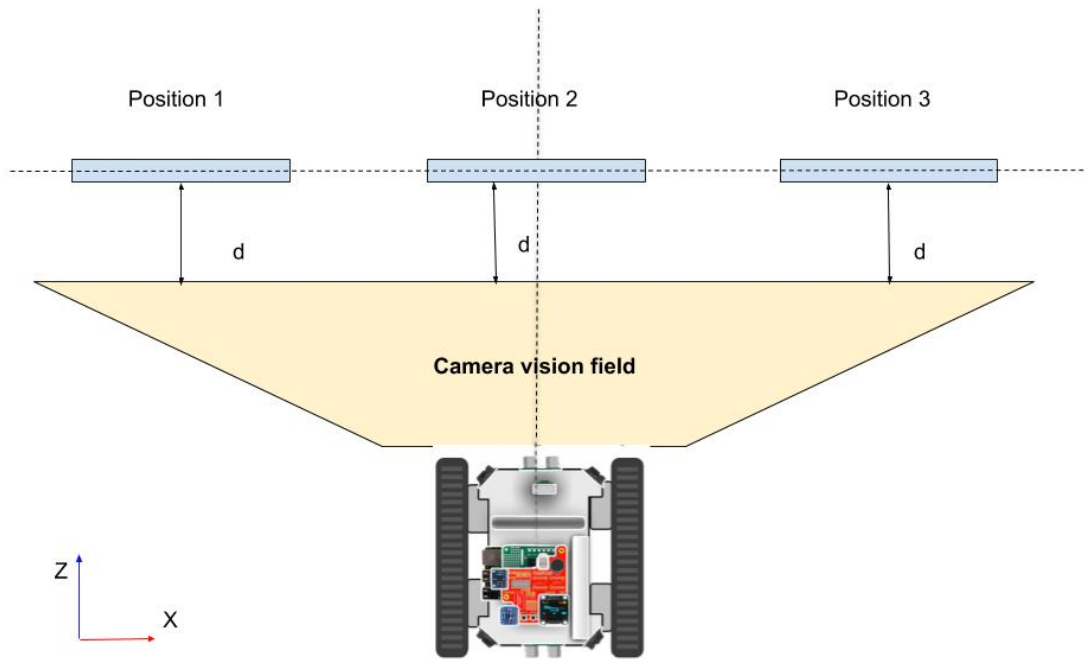


Figure 4.1: Camera vision field

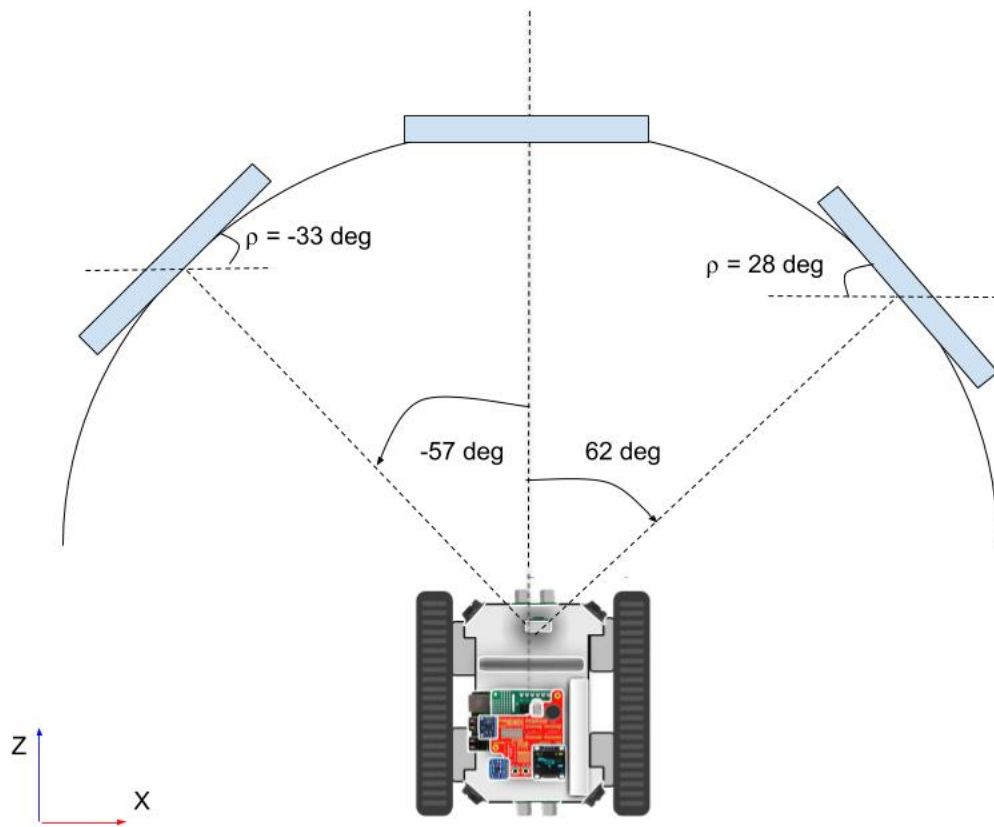


Figure 4.2: Limits of camera vision field



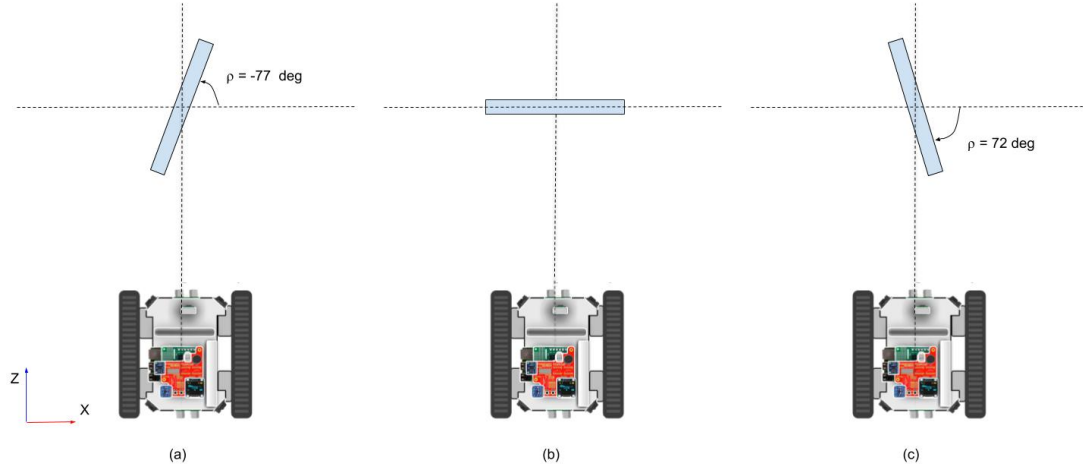


Figure 4.3: Maximum detectable rotations (a) counterclockwise, (b) no rotation and (c) clockwise

#### 4.4 Problems measuring distance traveled

There are no sensor mounted on the Rover that measures accurately of the distance traveled such as GPS or encoders. We are using ultrasonic sensor to measure the distance to the marker, however this approach only works when the rover leader in within 40cm radius and its orientation is not greater than 30 degrees given the way that sensors works. For angles greater than 30 degrees the bounced waved is not detectable. Due to the previous explained reasons and the fact it is know the estimated distance to the marker, the use of a sensor to measure distance travelled is needed, and also it will broad the range of possible applications.

In addition, sometimes the follower is not able to detect the marker anymore since it is very close to it due to our system does not measure accurately the distance travelled. An example is shown in 4.4. It is observed that at the final position  $d = 3cm$ , the follower lost track of the marker.

#### 4.5 Switching to Raspbian to AGL

The rover-app described in this document runs on top of the Raspbian operation system. In further improvements the application should run on AGL. However, the current version of the Eclipse Kuksa software development kit (SDK) is not compatible with `OpenCV 3.4.1`, thus this issue should be addressed first.

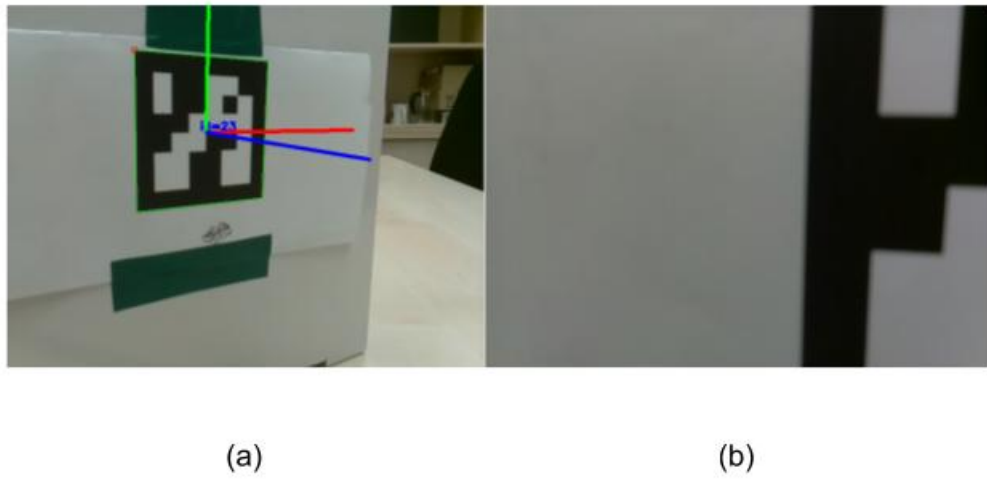


Figure 4.4: (a) Initial position  $d = 22.73cm$ ,  $\rho = -33.41^\circ$  (b) Final Position

# Conclusions

The design and development of a rover-app has been presented. The application allows a Rover to follow without human intervention a visual marker on another Rover. The described rover-app is based on `OpenCV` libraries and rover-services to interface with camera, motors and sensors mounted on Rover.

Our experimental results show the high accuracy of our application to estimate the distance to the marker, and the existence of an almost constant error in the angle estimation. Moreover, we presented some challenges and issues related to our application, and how to address them in future versions.

# List of Tables

2.1	Most importante requirements . . . . .	7
2.2	Statistics of estimated Euler angles and distance to visual marker . . . . .	14
3.1	Initial settings and estimations . . . . .	20
3.2	Measurements and final estimations . . . . .	21
3.3	Accuracy comparison between ultrasonic ranging module HC-SC04 readings and PiCamera estimations. . . . .	21

# List of Figures

1.1	Eclipse Kuksa Ecosystem [12]	4
1.2	Rover Components [1]	5
2.1	Rover Use Case	9
2.2	The pinhole imaging model [8].	9
2.3	Planar Patterns [3]	10
2.4	Some camera views used for calibration	11
2.5	Camera axis	14
2.6	Angles in X-axis $\psi$ , Y-axis $\rho$ and Z-axis $\phi$	15
2.7	Rotation rotations (a) Rotation in X-axis (b) Rotation in Y-axis	16
2.8	Activity diagram	18
4.1	Camera vision field	23
4.2	Limits of camera vision field	23
4.3	Maximum detectable rotations (a) counterclockwise, (b) no rotation and (c) clockwise	24
4.4	(a) Initial position $d = 22.73cm$ , $\rho = -33.41^\circ$ (b) Final Position	25

# Bibliography

- [1] Eclipse APP4MC. Eclipse app4mc - rover documentation, 2017.  
URL: <https://app4mc-rover.github.io/rover-docs/>.
- [2] Eclipse APP4MC. Rover api documentation, 2017.  
URL: <https://app4mc-rover.github.io/rover-app/>.
- [3] G. Bradski. The OpenCV Library. *Dr. Dobb's Journal of Software Tools*, 2000.
- [4] Pedro Cuadra. Raml to agl, 2017.  
URL: <https://github.com/pjcuadra/raml2agl>.
- [5] David A. Forsyth and Jean Ponce. *Computer Vision: A Modern Approach*. Prentice Hall Professional Technical Reference, 2002.
- [6] The Linux Foundation. Automotive grade linux, 2016.  
URL: <https://www.automotivelinux.org/>.
- [7] Gregory G. Slabaugh. Computing euler angles from a rotation matrix, 01 1999.  
Technical Report URL: [www.gregslabaugh.net/publications/euler.pdf](http://www.gregslabaugh.net/publications/euler.pdf).
- [8] Rafael Garcia. *A proposal to estimate the motion of an underwater vehicle through visual mosaicking*. PhD thesis, University of Girona. Doctor of Philosophy Girona, 2001.
- [9] J.Y.Bouguet. Matlab calibration tool (2018-11-20).  
URL:<http://www.vision.caltech.edu/bouguetj/calibdoc/>.
- [10] McKinsey and Company. A road map to the future for the auto industry, 2014.  
URL: <https://www.mckinsey.com/industries/automotive-and-assembly/our-insights/a-road-map-to-the-future-for-the-auto-industry>.
- [11] McKinsey and Company. What's driving the connected car, 2014.  
URL: <https://www.mckinsey.com/industries/automotive-and-assembly/our-insights/whats-driving-the-connected-car>.
- [12] APPSTACLE Project. Eclipse kuksa, 2016.  
URL: <https://www.eclipse.org/kuksa/>.

- [13] APPSTACLE Project. open standard application platform for cars and transportation vehicles, 2016.  
URL: <https://itea3.org/project/appstacle.html>.
- [14] Richard Szeliski. *Computer Vision: Algorithms and Applications*. Springer-Verlag, Berlin, Heidelberg, 1st edition, 2010.
- [15] Z. Zhang. Emerging topics in computer vision, chapter 2: Camera calibration. Upper Saddle River, NJ, USA, 2004. Prentice Hall PTR.
- [16] Zhengyou Zhang. A flexible new technique for camera calibration. *IEEE Trans. Pattern Anal. Mach. Intell.*, 22(11):1330–1334, November 2000.

## Appendix A

# Appendix

### A.1 Calibration of the picam in raspbian

The `OpenCV` version we are using is 3.4.1.

bla bla bla... more details here

### A.2 Answer to the “Life, the Universe, and All” questions

A Pitagorasz-tételből levezetve

$$c^2 = a^2 + b^2 = 42.$$

A Faraday-indukciós törvényből levezetve

$$\text{rot} E = -\frac{dB}{dt} \quad \longrightarrow \quad U_i = \oint_{\mathbf{L}} \mathbf{E} d\mathbf{l} = -\frac{d}{dt} \int_A \mathbf{B} d\mathbf{a} = 42.$$